J. Fluid Mech. (1989), *vol.* 209, *pp.* 521–542
Printed in Great Britain

The instability of a dispersion of sedimenting spheroids

By DONALD L. KOCH[1] AND ERIC S. G. SHAQFEH[2]

[1] School of Chemical Engineering, Cornell University, Ithaca, NY 14853, USA

[2] AT & T Bell Laboratories, 600 Mountain Avenue, Murray Hill, NJ 07974, USA

(Received 29 July 1988 and in revised form 2 May 1989)

It is shown that hydrodynamic interactions between non-Brownian, non-spherical, sedimenting particles give rise to an increase in the number of neighbouring particles in the vicinity of any given particle. This result suggests that the suspension is unstable to particle density fluctuations even in the absence of inertia; a linear stability analysis confirms this inference. It is argued that the instability will lead to convection on a lengthscale $(nl)^{-\frac{1}{2}}$, where l is a characteristic particle length and n is the particle number density. Sedimenting suspensions of spherical particles are shown to be stable in the absence of inertial effects.

1. Introduction

The mean sedimentation velocity in a suspension of non-spherical particles, such as the spheroidal particles treated in this paper, depends strongly on the suspension structure. The sedimentation velocity U^s of a non-spherical particle depends on its orientation, varying by an $O(U^s)$ amount as its orientation changes. Each particle rotates under the influence of the fluid velocity fluctuations resulting from the settling of the surrounding particles. The particle orientation distribution is determined by these interparticle hydrodynamic interactions, unless the particles are weighted such that they seek a preferred orientation.

Recently, the effects of hydrodynamic interactions on the orientation of freely suspended particles flowing through fixed beds have been analysed by Shaqfeh & Koch (1988). In that instance, it was demonstrated that the particle orientations were determined primarily by long-range interactions. Each long-range interaction between a freely suspended particle and a fixed particle causes a small change in orientation. As a result the bed-average orientation distribution evolves in a diffusive manner, satisfying a local orientational advection–diffusion equation. The orientational 'advection' results from a drift velocity associated with rotational dilatation. The orientational diffusivity created by interactions between the fixed and freely suspended particles was demonstrated to be an average rotational velocity correlation function relating the rotational velocity of a freely suspended particle at a point in the bed, to its rotation rate at all previous points along a particle path. Both the 'drift' velocity and the diffusivity were calculated explicitly for a wide class of axisymmetric particles and analytic solutions were obtained for the bed average orientation distribution function at steady state.

It would be desirable to apply a similar analysis to calculate the *orientation* distribution in a sedimenting suspension of non-spherical particles. It will be shown, however, that such a straightforward application does not exist, primarily because

of the long-range nature of the hydrodynamic interparticle interactions. If the velocity disturbance caused by a sedimenting spheroid is approximated by a Stokeslet, the rotation rate of one particle due to a second decays like r^{-2} as the radial interparticle separation r goes to infinity. Therefore, the integral along a trajectory of a particle's past rotations resulting from its interactions with a second particle decays like r^{-1} as $r \to \infty$. As a result the deviation of the joint probability density for the position and orientation of the two particles from its asymptotic value also decays like r^{-1}. It follows that if one attempts to evaluate the effective rotatory diffusivity in a random suspension by summing the contribution of each 'second' particle to the integral along a trajectory of the rotation rate correlation function one obtains a conditionally convergent integral as $r \to \infty$. It is not possible, then, to evaluate the orientation distribution or the mean sedimentation velocity in a suspension of non-spherical particles, unless some account is taken of the effect of non-uniformities in the particle distribution on the fluid velocity perturbations. Similar divergence problems have been shown to arise in an attempt to calculate the variance of the sedimentation velocity in a sedimenting suspension of spheres of uniform probability (Caflisch & Luke 1985).

If the non-uniformity of the particle distribution that developed as a result of particle interactions consisted of a net deficit of particles in the neighbourhood of each particle, one might expect the velocity fluctuations in the dispersion to be less than those in a uniform dispersion. However, it will be shown in §2 that, in the case of sedimenting spheroids, hydrodynamic interactions lead to a net excess of particles in the vicinity of each particle. In §3, we show that the tendency for long-range density increases (or 'clumping') in sedimenting suspension of spheroids causes an instability and the suspension ceases to be homogeneous (on scales of $O((nl)^{-\frac{1}{2}})$ where l is a characteristic particle length and n is the particle number density). The possibility of such an instability occurring in suspensions of spherical particles is investigated in §4, where we demonstrate that, including pairwise particle interactions, such a suspension is neutrally stable to density perturbations (in the absence of damping forces such as Brownian motion).

2. The effect of two spheroid interactions on the pair probability

In this section we consider the dynamic interactions between two sedimenting spheroidal particles. We are particularly interested in determining whether these interactions tend to create an increase or deficit in the number density of neighbouring particles.

In a pure fluid, spheroidal particles will sediment at a velocity U_i^s, which depends on the orientation, p_i, of their axes of rotational symmetry. For convenience, we have adopted Einstein vector notation with δ_{j3} indicating the unit vector in the direction of gravity. In general, U_i^s is given by (Overbeck 1876; Happel & Brenner 1965)

$$U_i^s = \delta_{j3}(\beta_0 \delta_{ij} + \beta_1 p_i p_j), \tag{2.1a}$$

where, for prolate spheroids, $\gamma > 1$,

$$\beta_0 = \frac{f}{16\pi\mu l}\left(\frac{\gamma^2}{\gamma^2-1} + \frac{2\gamma^3-3\gamma}{(\gamma^2-1)^{\frac{3}{2}}}\ln\left[\gamma+(\gamma^2-1)^{\frac{1}{2}}\right]\right), \tag{2.1b}$$

$$\beta_1 = \frac{f}{16\pi\mu l}\left(\frac{-3\gamma^2}{\gamma^2-1} + \frac{2\gamma}{(\gamma^2-1)^{\frac{3}{2}}}\ln\left[\gamma+(\gamma^2-1)^{\frac{1}{2}}\right] + \frac{\gamma-2\gamma^3}{(\gamma^2-1)^{\frac{3}{2}}}\ln\left[\gamma-(\gamma^2-1)^{\frac{1}{2}}\right]\right), \tag{2.1c}$$

and, for oblate spheroids, $\gamma < 1$,

$$\beta_0 = \frac{f}{16\pi\mu l}\left(\frac{-\gamma^2}{1-\gamma^2} + \frac{3\gamma - 2\gamma^3}{(1-\gamma^2)^{\frac{3}{2}}}\arcsin(1-\gamma^2)^{\frac{1}{2}}\right), \tag{2.1d}$$

$$\beta_1 = \frac{f}{16\pi\mu l}\left(\frac{3\gamma^2}{1-\gamma^2} + \frac{2\gamma - 4\gamma^3}{(1-\gamma^2)^{\frac{3}{2}}}\arctan\left(\frac{(1-\gamma^2)^{\frac{1}{2}}}{\gamma}\right) - \frac{3\gamma - 2\gamma^3}{(1-\gamma^2)^{\frac{3}{2}}}\arcsin(1-\gamma^2)^{\frac{1}{2}}\right). \tag{2.1e}$$

Here, l is the semiaxis of the spheroid along the axis of rotational symmetry, and γ is the aspect ratio, l/a, where a is the semiaxis perpendicular to the axis of rotational symmetry. The constant β_0 is always positive for particles heavier than the surrounding fluid. On the other hand, for such heavy particles, β_1 is positive for prolate spheroids, negative for oblate spheroids, and zero for spheres. For our purposes, the most important characteristics of the sedimentation velocity as given by (2.1) are: (i) a spheroid falls faster when its 'thin' side is pointing in the direction of gravity; and (ii) the component of U_i^s perpendicular to gravity is non-zero when the spheroid's orientation, p_i, is at an oblique angle to gravity. Note that whereas two identical spherical particles do not move relative to one another, two non-spherical particles do sediment at different speeds and in general their relative speed is $O(U^s)$. Thus, typically one spheroid will sediment through the region surrounding a second spheroid thereby changing the orientations of both particles. Kim (1985) showed that pairs of spheroids may have closed trajectories, however these closed trajectories only occur for particles that are separated by a distance comparable to the length l. We are interested in the long-range structure of the pair probability, because, in a dilute suspension, the long-range interactions control the particle dynamics. Thus, we consider only those trajectories in which the particles remain separated by a distance large compared to their length l; Kim (1985) has shown that such trajectories are not closed.

Neglecting Brownian motion and the effects of interactions between three or more particles, the joint probability density $P(\boldsymbol{r}, \boldsymbol{p}^B; \boldsymbol{0}, \boldsymbol{p}^A)$ for finding two particles at a relative position $\boldsymbol{r}$ with orientations $\boldsymbol{p}^A$ and $\boldsymbol{p}^B$ satisfies the conservation equation:

$$\frac{\partial P}{\partial t} + \nabla\cdot(\boldsymbol{U}^r P) + \nabla_{p^A}\cdot(\dot{\boldsymbol{p}}^A P) + \nabla_{p^B}\cdot(\dot{\boldsymbol{p}}^B P) = 0, \tag{2.2}$$

where $\boldsymbol{U}^r$ and $\boldsymbol{r}$ are the velocity and position of particle B relative to particle A, $\dot{\boldsymbol{p}}^A$ and $\dot{\boldsymbol{p}}^B$ are the time rates of change of the particle orientations, and ∇_{p^A} and ∇_{p^B} are the Nablé operators with derivatives taken with respect to $\boldsymbol{p}^A$ and $\boldsymbol{p}^B$. At sufficiently large separations the orientations and positions of the particles are uncorrelated, so $P \sim n^2 \Psi(\boldsymbol{p}^A)\,\Psi(\boldsymbol{p}^B)$ as $r \to \infty$, where Ψ is the average orientation distribution in the suspension.

As we are only interested in the interactions between well-separated particles, i.e. $rl^{-1} \gg 1$, we may neglect the direct effects of hydrodynamic interactions on the relative velocity, which decay like $l^4 r^{-4}$. The relative velocity, U_i^r, is then approximately the difference between the two particles' settling velocities in a pure Newtonian fluid, and from (2.1), we obtain

$$U_i^r = \beta_1(p_i^B p_j^B - p_i^A p_j^A)\,\delta_{j3}. \tag{2.3}$$

Note that, in fact, we have only neglected the *direct* influence of interactions on the relative velocity, and each particle will still create a velocity disturbance in the fluid which will cause the other to rotate and will in turn affect their relative velocity. The

large interparticle separation enables us to make three approximations in determining the particles' rotation rates: (i) hydrodynamic reflections may be neglected as their effects will be of higher order in lr^{-1}; (ii) the velocity disturbance that one particle causes in the vicinity of the second may be approximated as that due to a point force; and (iii) this velocity disturbance may be treated as linear shearing motion on lengths comparable with that of the second particle. Using these approximations, the rotation rates are given by the well-known relations (Bretherton 1962; Jeffery 1923):

$$\dot{p}_i^{\mathrm{B}} = (\delta_{ij} - p_i^{\mathrm{B}} p_j^{\mathrm{B}}) p_k^{\mathrm{B}} \left[\left(\frac{\gamma^2 - 1}{\gamma^2 + 1} \right) E_{jk} + W_{jk} \right], \tag{2.4a}$$

$$\dot{p}_i^{\mathrm{A}} = -(\delta_{ij} - p_i^{\mathrm{A}} p_j^{\mathrm{A}}) p_k^{\mathrm{A}} \left[\left(\frac{\gamma^2 - 1}{\gamma^2 + 1} \right) E_{jk} + W_{jk} \right], \tag{2.4b}$$

where

$$\boldsymbol{E} = \tfrac{1}{2}(\nabla \boldsymbol{u} + \nabla \boldsymbol{u}^{+}), \quad \boldsymbol{W} = \tfrac{1}{2}(\nabla \boldsymbol{u}^{+} - \nabla \boldsymbol{u}), \tag{2.4c, d}$$

$\boldsymbol{u}$ is the velocity field at a position $\boldsymbol{r}$ due to a point force of magnitude $f = \Delta\rho V_{\mathrm{p}} g$ located at the origin. Here, $\Delta\rho$ is the difference between the densities of the particles and fluid and V_{p} is the particle volume. The minus sign in (2.4b) arises because the position of particle A relative to B is $-\boldsymbol{r}$ and the velocity gradient due to a point force is an odd function of position. When the particle separation is in the range $l \ll r \ll (nl)^{-\frac{1}{2}}$, the velocity disturbance of each particle may be approximated as the velocity due to a Stokeslet, which satisfies (Saffman 1973):

$$-\mu \nabla^2 \boldsymbol{u} + \nabla p = \boldsymbol{f} \delta(\boldsymbol{r}), \tag{2.5a}$$

$$\nabla \cdot \boldsymbol{u} = 0. \tag{2.5b}$$

The restriction to separations less than $(nl)^{-\frac{1}{2}}$ arises because for larger separations one must take into account the effect of changes in the number of neighbouring particles on the velocity disturbance.

We may obtain the joint probability density $P(\boldsymbol{r}, \boldsymbol{p}^{\mathrm{B}}; \boldsymbol{0}, \boldsymbol{p}^{\mathrm{A}})$ from (2.2) with the particles' relative velocity given by (2.3) and their rotation rates by (2.4). The rotation rates (2.4) are proportional to the velocity gradient which decays like $l^2 r^{-2}$ as $r \to \infty$. The total change in a particle's orientation during an interaction involves an integral along its trajectory of the particle's rotation rate, and thus, this change decays like lr^{-1}. Therefore, for $rl^{-1} \gg 1$, the changes in the particles' orientations are small, so the difference between the joint probability density and its asymptotic value, i.e. $P' \equiv P - n^2 \Psi(\boldsymbol{p}^{\mathrm{A}}) \Psi(\boldsymbol{p}^{\mathrm{B}})$ is small like lr^{-1}. Neglecting terms smaller than $l^2 r^{-2}$ as $r \to \infty$, (2.2) becomes at steady state:

$$\boldsymbol{U}^{\mathrm{r}} \cdot \nabla P' = -\nabla_{p^{\mathrm{A}}} \cdot [\dot{\boldsymbol{p}}^{\mathrm{A}} n^2 \Psi(\boldsymbol{p}^{\mathrm{A}}) \Psi(\boldsymbol{p}^{\mathrm{B}})] - \nabla_{p^{\mathrm{B}}} \cdot [\dot{\boldsymbol{p}}^{\mathrm{B}} n^2 \Psi(\boldsymbol{p}^{\mathrm{A}}) \Psi(\boldsymbol{p}^{\mathrm{B}})]. \tag{2.6}$$

Equation (2.6) may be solved upon Fourier transformation to give

$$\hat{P}' = -\frac{1}{2\pi i \boldsymbol{k} \cdot \boldsymbol{U}^{\mathrm{r}}} [\nabla_{p^{\mathrm{A}}} \cdot (\hat{\dot{\boldsymbol{p}}}^{\mathrm{A}} n^2 \Psi(\boldsymbol{p}^{\mathrm{A}}) \Psi(\boldsymbol{p}^{\mathrm{B}})) + \nabla_{p^{\mathrm{B}}} \cdot (\hat{\dot{\boldsymbol{p}}}^{\mathrm{B}} n^2 \Psi(\boldsymbol{p}^{\mathrm{A}}) \Psi(\boldsymbol{p}^{\mathrm{B}}))]. \tag{2.7}$$

The transforms $\hat{\dot{\boldsymbol{p}}}^{\mathrm{A}}$ and $\hat{\dot{\boldsymbol{p}}}^{\mathrm{B}}$ are related to $\hat{\boldsymbol{E}}$ and $\hat{\boldsymbol{W}}$ by (2.4a, b). $\hat{\boldsymbol{E}}$ and $\hat{\boldsymbol{W}}$ are just the transforms of the symmetric and antisymmetric parts of the gradient of the velocity disturbance due to a particle and the latter is given by the solution in Fourier space of (2.5), i.e.

$$\hat{\boldsymbol{u}}(\boldsymbol{k}) = \frac{\left(\boldsymbol{I} - \dfrac{\boldsymbol{k}\boldsymbol{k}}{k^2} \right) \cdot \boldsymbol{f}}{\mu (2\pi k)^2}. \tag{2.8}$$

Equation (2.7) simply represents the transform of the integral of the right-hand side of (2.6) along a particle trajectory.

The joint probability density for finding a particle of any orientation at $\boldsymbol{r}$ and a particle of orientation $\boldsymbol{p}^{\mathrm{A}}$ at the origin is:

$$n\Psi(\boldsymbol{p}^{\mathrm{A}})\, g(\boldsymbol{r}\,|\,\mathbf{0},\boldsymbol{p}^{\mathrm{A}}) = \int \mathrm{d}\boldsymbol{p}^{\mathrm{B}} P(\boldsymbol{r},\boldsymbol{p}^{\mathrm{B}};\mathbf{0},\boldsymbol{p}^{\mathrm{A}}). \tag{2.9}$$

where the pair probability g is the probability density for finding a particle of any orientation located at $\boldsymbol{r}$, when a particle of specified orientation $\boldsymbol{p}^{\mathrm{A}}$ is located at $\mathbf{0}$.

Thus, the extra particle density ρ, the difference between the pair probability g and number density n, is given by

$$\rho(\boldsymbol{r}\,|\,\mathbf{0},\boldsymbol{p}^{\mathrm{A}}) = \frac{1}{n\Psi(\boldsymbol{p}^{\mathrm{A}})} \int \mathrm{d}\boldsymbol{p}^{\mathrm{B}} P'(\boldsymbol{r},\boldsymbol{p}^{\mathrm{B}};\mathbf{0},\boldsymbol{p}^{\mathrm{A}}). \tag{2.10}$$

The excess particle density ρ (like P') decays like lr^{-1}. Because of this slow decay, the total excess (or deficit) of particles within a radial distance R of a given particle obtained by integrating ρ over this volume is $O(1)$, when $R \approx O((nl)^{-\frac{1}{2}})$. On this lengthscale one can no longer neglect the effects of the change in the particle density on the velocity disturbance.

We wish to determine the sign of the net change in the number of particles within a sphere of radius R of a given particle, where $l \ll r \ll (nl)^{-1}$. This net change, which we shall call H, is given by

$$H \equiv \int_{r \leqslant R} \mathrm{d}\boldsymbol{r}\, \rho(\boldsymbol{r}\,|\,\mathbf{0},\boldsymbol{p}^{\mathrm{A}}). \tag{2.11}$$

We shall determine the sign of H for a spherical volume of radius R, where $l \ll R \ll (nl)^{-\frac{1}{2}}$. On a lengthscale R the effect of the particle density change on the velocity disturbance may be neglected. On the lengthscale $(nl)^{-\frac{1}{2}}$, the coupling between the particle density and the velocity fluctuations becomes significant. If H is positive, one may expect the homogeneous suspension to be unstable to particle density perturbations on this lengthscale.

Equation (2.11) can be written in terms of a volume integral over all space using (2.10) and the 'ball' function $\Pi(r/2R)$ of Bracewell (1978), to give

$$H = \frac{1}{n\Psi(\boldsymbol{p}^{\mathrm{A}})} \int \mathrm{d}\boldsymbol{p}^{\mathrm{B}} \int \mathrm{d}\boldsymbol{r}\, \Pi\left(\frac{r}{2R}\right) P'(\boldsymbol{r},\boldsymbol{p}^{\mathrm{B}};\mathbf{0},\boldsymbol{p}^{\mathrm{A}}), \tag{2.12}$$

where the 'ball' function $\Pi(r/2R)$ is equal to 1 for $r < R$ and is equal to 0 otherwise. Applying the convolution theorem, (2.12) becomes

$$H = \frac{1}{n\Psi(\boldsymbol{p}^{\mathrm{A}})} \int \mathrm{d}\boldsymbol{p}^{\mathrm{B}} \int \mathrm{d}\boldsymbol{k}\, \hat{\Pi}(-\boldsymbol{k})\, \hat{P}'(\boldsymbol{k}), \tag{2.13}$$

where the Fourier transform of the 'ball' function is (Bracewell 1978) given by

$$\hat{\Pi}(\boldsymbol{k}) = \frac{\sin(2\pi kR) - 2\pi kR\cos(2\pi kR)}{2\pi^2 k^3 R^3}. \tag{2.14}$$

For simplicity we shall consider an isotropic bulk orientation distribution $\Psi = (4\pi)^{-1}$. Substituting (2.7) and (2.14) into (2.13), we obtain

$$H = \frac{3nf}{8\pi\mu}\left(\frac{\gamma^2-1}{\gamma^2+1}\right)\int d\boldsymbol{p}^B \int d\boldsymbol{k}\left[\frac{\sin(2\pi kR)-2\pi kR\cos(2\pi kR)}{8\pi^4 k^5 R^3}\right] \times\left[\frac{p_i^B p_j^B - p_i^A p_j^A}{\kappa_l U_l^r}\right]\kappa_i(\delta_{jk}-\kappa_j\kappa_k)\,\delta_{k3}, \quad (2.15)$$

where $\kappa_i \equiv k_i/k$, and we have used (2.4) for the particle rotation rates and (2.8) for the velocity disturbance. Recall that the relative velocity $\boldsymbol{U}^r$ is given by (2.3). Performing the integration in k and rearranging, (2.15) becomes

$$H = \frac{3\pi fR^2}{32\pi^2\mu}\left(\frac{\gamma^2-1}{\gamma^2+1}\right)\int d\boldsymbol{p}^B \int \sin\Theta\, d\Theta\, d\Phi \times\left[\frac{(p_i^B p_j^B - p_i^A p_j^A)\kappa_i\delta_{j3}}{\beta_1(p_l^B p_m^B - p_l^A p_m^A)\kappa_l\delta_{m3}} - \frac{\kappa_i\kappa_j\kappa_k\delta_{k3}(p_i^B p_j^B - p_i^A p_j^A)}{\kappa_l U_l^r}\right], \quad (2.16)$$

where Θ and Φ are the angular variables in a spherical coordinate system in Fourier space. The first term in the integrand in (2.16) is imply $1/\beta_1$ and may be integrated easily in Θ and Φ to give $4\pi/\beta_1$. The second term in (2.16) may be integrated, using the relation

$$\int \sin\Theta\, d\Theta\, d\Phi \frac{\kappa_i\kappa_j\kappa_k}{U_l^r\kappa_l} = \frac{4\pi}{3U^{r^2}}(U_i^r\delta_{jk}+U_j^r\delta_{ik}+U_k^r\delta_{ij}) - \frac{8\pi}{3U^{r^4}}U_i^r U_j^r U_k^r, \quad (2.17)$$

to give

$$H = \frac{3nfR^2}{4\mu\beta_1}\left(\frac{\gamma^2-1}{\gamma^2+1}\right)\left[\tfrac{1}{3}+\frac{1}{6\pi}\int d\boldsymbol{p}^B \frac{\beta_1^4[(p_3^B)^2-(p_3^A)^2]^2[1-(p_i^A p_i^B)^2]}{U^{r^4}}\right]. \quad (2.18)$$

The integral in (2.17) contains a factor $(U_l^r\kappa_l)^{-1}$, and thus appears superficially to be conditionally convergent near points where $U_l^r\kappa_l = 0$. However, the Fourier transform $(U_l^r\kappa_l)^{-1}$ is a generalized function and its integral is defined to be the Cauchy principal value (Lighthill 1980). Equation (2.18) can be derived without the requirement of integrating generalized functions if the pair probability is evaluated by using the method of characteristics in real space. The real-space analysis is available by request from the authors.

From (2.18) it is clear that H is positive. The first term in the square brackets is positive and the integrand of the second term is non-negative for all values of $\boldsymbol{p}^A$ and $\boldsymbol{p}^B$. This indicates that two-particle interactions lead to an *increase* in the neighbouring particles near a given particle. Note that this result is independent of whether the spheroids are prolate or oblate, the factor $(\gamma^2-1)/[(\gamma^2+1)\beta_1]$ being positive for both prolate and oblate spheroids.

The integrand of the second term in the expression (2.18) for the excess number of neighbouring particles, H, becomes singular when the magnitude of the relative velocity U^r goes to zero. The relative velocity may go to zero in two cases: (i) when the two orientations are identical, $p_i^A = p_i^B$, or (ii) when both orientations are perpendicular to gravity, $p_3^A = p_3^B = 0$. Consider first case (i) and denote the angle between $\boldsymbol{p}^B$ and $\boldsymbol{p}^A$ as Θ_{BA}. The denominator of the integrand is then $O((\Theta_{BA})^4)$ while the numerator is $O((\Theta_{BA})^3)$ as $\Theta_{BA}\to 0$. Thus we obtain an area integral over the unit sphere in $\boldsymbol{p}^B$ of a quantity that is singular like $(\Theta_{BA})^{-1}$ and so we do not obtain a large contribution to H from case (i). On the other hand case (ii) does yield a large $O[(p_3^A)^{-1}]$

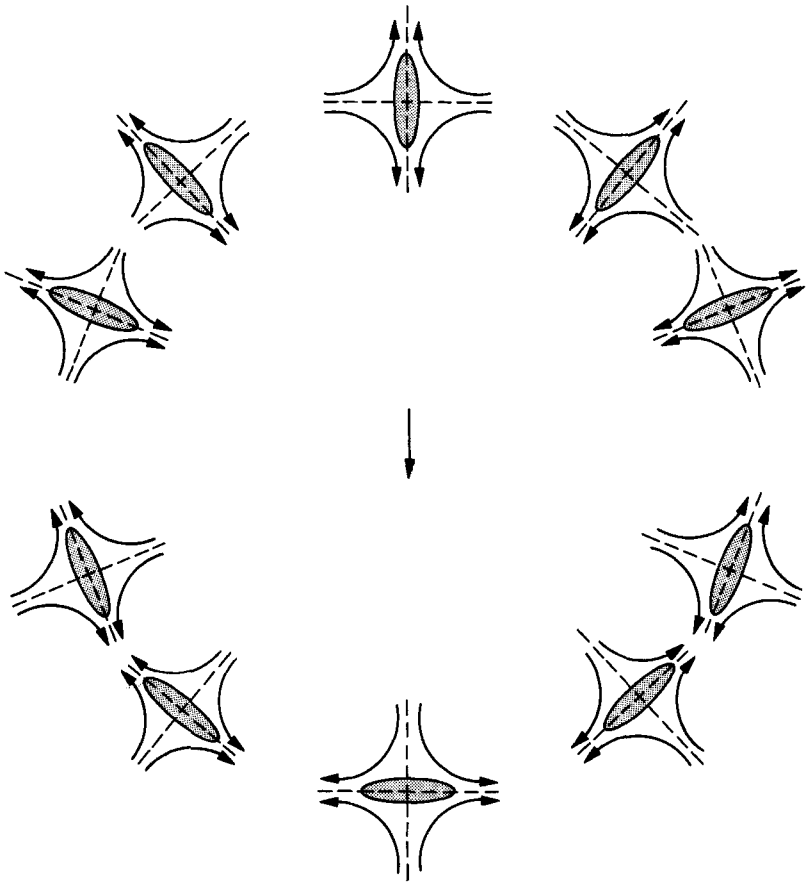

FIGURE 1. The effect of a point-force velocity disturbance on the orientation of surrounding particles is shown schematically. The streamlines corresponding to the symmetric part of the local, linear shear field near each neighbouring particle are illustrated. The neighbouring particles are drawn in the most favoured orientation – the orientation at which particle density is being increased most rapidly by the point-force velocity disturbance.

contribution to the excess of particles neighbouring a particle that is oriented nearly perpendicular to gravity, i.e. $p_3^A \ll 1$. In the limit $p_3^A \to 0$ one obtains unbounded contributions to H from other horizontally oriented particles in the present approximation. In this limit the approximation that the change in particle orientation in a single 'collision' is small breaks down and P' is no longer small. However, none of these considerations alter the result that H is positive indicating an excess of near neighbours.

Figure 1 illustrates how a net increase in the number of neighbouring particles is created. With the aforementioned approximations, any given particle creates a point force velocity disturbance. The neighbouring particles tend to align with their 'thin' sides parallel to the direction of the extensional component of the fluid motion caused by the point force. The principal axis of extension is always parallel to the radial vector, but above the point force the flow converges while below it diverges. Thus, the particles above the point force tend to align with their 'thin' sides parallel to gravity and those below tend to align perpendicular to gravity. It follows that the particles above a given particle tend to fall faster than those below, leading to a net tendency for particles to accumulate in the vicinity of any particular particle.

The tendency for sedimenting spheroids to aggregate during the sedimentation process strongly suggests that a homogeneous sedimenting suspension may be unstable to particle number density fluctuations. Any positive density fluctuation creates a velocity disturbance which may, through its effect on the orientation of neighbouring spheroids, be expected to enhance the density fluctuation. The stability of a homogeneous, sedimenting suspension of spheroids is investigated more carefully in the following section.

3. Stability of a homogeneous suspension of spheroidal particles

In this section we consider the stability of a homogeneous suspension of sedimenting spheroids to small amplitude fluctuations in particle number density. We demonstrated in the preceding section that two particle interactions tend on average to cause particles to clump together, suggesting that the homogeneous suspension may be unstable.

At present, we consider a suspension that is sufficiently dilute so that particle interactions may be neglected in comparison with the interaction of the particle with a bulk disturbance. Thus, we consider the evolution of the bulk particle density or concentration $c(\boldsymbol{x},\boldsymbol{p})$, which satisfies the particle conservation equation:

$$\frac{\partial c}{\partial t}+\nabla_{\mathrm{p}}\cdot(\dot{\boldsymbol{p}}c)+\nabla\cdot(\boldsymbol{U}c)=0, \tag{3.1}$$

where $\boldsymbol{U}(\boldsymbol{x})$ is the velocity of a particle at position $\boldsymbol{x}$. In the dilute limit $\boldsymbol{U}$ is a sum of the average fluid velocity $\langle\boldsymbol{u}\rangle$ caused by all of the particles in the suspension and the sedimentation velocity (2.1) in a quiescent, pure fluid. Here $\langle\ \rangle$ indicates an ensemble average over all the possible configurations of the suspension. The particle rotation rate $\dot{\boldsymbol{p}}$ is given by (2.4a, c, d) with the fluid velocity now being the bulk average $\langle\boldsymbol{u}\rangle$.

To calculate the average fluid velocity field, we shall use a point-particle approximation. This approximation is valid when the wavelength k^{-1} of the disturbance introduced in (3.5) is much larger than the particle size l, so that most of the particles causing the velocity disturbance at position $\boldsymbol{x}$ are a large distance away from $\boldsymbol{x}$. The fluid velocity field in the point-particle approximation satisfies (Saffman 1973):

$$-\mu\nabla^2\boldsymbol{u}+\nabla p^*=\sum_{i=1}^{N}\boldsymbol{f}\delta(\boldsymbol{x}-\boldsymbol{R}_i), \tag{3.2a}$$

$$\nabla\cdot\boldsymbol{u}=0, \tag{3.2b}$$

where $\boldsymbol{R}_i$ is the position of the ith particle, p^* is the dynamic pressure, and $\boldsymbol{f}=V_{\mathrm{p}}\Delta\rho\boldsymbol{g}$ is the force of gravity acting on each particle. In the point-particle approximation, Batchelor's (1972) renormalization is equivalent to adjusting the reduced pressure $p\equiv p^*-nfz$ to reflect the increase in the average density of the suspension due to the presence of the particles. In this section n will be used to denote the volume averaged particle number density, which may differ from the local number density, $\int \mathrm{d}\boldsymbol{p}\,c$, owing to the particle density perturbations. Substituting the adjusted reduced pressure into (3.2a) yields:

$$-\mu\nabla^2\boldsymbol{u}+\nabla p=\boldsymbol{f}\left[\sum_{i=1}^{N}\delta(\boldsymbol{x}-\boldsymbol{R}_i)-n\right]. \tag{3.3}$$

The equations for the bulk fluid average velocity and pressure fields are obtained by taking the unconditional ensemble average of (3.3) and (3.2*b*) to give

$$-\mu\nabla^2\langle\boldsymbol{u}\rangle+\nabla\langle p\rangle=\boldsymbol{f}\left[-n+\int d\boldsymbol{p}\,c(\boldsymbol{x},\boldsymbol{p})\right],\quad \nabla\cdot\langle\boldsymbol{u}\rangle=0. \tag{3.4a, b}$$

The base state for the stability analysis is a homogeneous suspension with a particle orientation distribution $\Psi(\boldsymbol{p})$, i.e. $c(\boldsymbol{x},\boldsymbol{p})=n\Psi(\boldsymbol{p})$. This spatially homogeneous particle density does not drive any bulk fluid motion (cf. equation (3.4), so $\langle\boldsymbol{u}\rangle=0$. Furthermore, since the bulk velocity is zero, the mean particle rotation rate $\dot{\boldsymbol{p}}$ is zero and the particle conservation equation (3.1) is satisfied for any orientation distribution. Note that in the present approximation we have not included the effects of particle interactions on the particle orientation.

We now consider the imposition of a normal-mode perturbation in number density of small amplitude ϵ on the spatially homogeneous state, i.e.

$$c(\boldsymbol{x},\boldsymbol{p},t)=n\Psi(\boldsymbol{p})+\epsilon nc'(\boldsymbol{k},\boldsymbol{p},\omega)\,e^{i\omega t}e^{i\boldsymbol{k}\cdot\boldsymbol{x}}. \tag{3.5}$$

Thus, the number density perturbations are plane waves of wavenumber $\boldsymbol{k}$. The suspension will be unstable and certain types of number density perturbations will grow, if there exists a perturbation for which the frequency $\omega\equiv\omega_R+i\omega_I$ has a negative imaginary part ω_I.

The small perturbation in particle number density drives a small velocity field

$$\langle\boldsymbol{u}\rangle=\epsilon n\boldsymbol{u}'\,e^{i\omega t}e^{i\boldsymbol{k}\cdot\boldsymbol{x}}. \tag{3.6a}$$

Substituting (3.6*a*) into (3.4) and solving for the velocity $\boldsymbol{u}'$, using the continuity condition to eliminate the pressure, we obtain

$$\boldsymbol{u}'(\boldsymbol{k},\omega)=\frac{\left(\boldsymbol{I}-\dfrac{\boldsymbol{kk}}{k^2}\right)\cdot\boldsymbol{f}}{\mu k^2}\int d\boldsymbol{p}\,c'. \tag{3.6b}$$

Since we are completely neglecting inertial effects the velocity field at any point in time is determined solely by the disturbance in particle density at that particular time. The small fluid velocity perturbation gives rise to a small rotary motion of the particles, which is obtained by substituting (3.6) into (2.4*a*, *c*, *d*) to give

$$\dot{p}_i=\epsilon n\dot{p}_i'\,e^{i\omega t}e^{i\boldsymbol{k}\cdot\boldsymbol{x}}, \tag{3.7a}$$

where

$$\dot{p}_i'=i(\delta_{ij}-p_ip_j)p_k\left[\frac{\gamma^2}{\gamma^2+1}k_k u_j'-\frac{1}{\gamma^2+1}u_k'k_j\right]. \tag{3.7b}$$

In writing (3.7*b*) we have used the stipulation that the wavelength of the perturbation is much larger than the particle length l to approximate the particles' rotation rate as that arising from a local, linear shear field.

Substituting (3.5), (3.6*a*), 3.7*a*) and (2.1) into the particle conservation equation (3.1), we obtain

$$\epsilon n\,e^{i\omega t}e^{i\boldsymbol{k}\cdot\boldsymbol{x}}[i\omega c'+\boldsymbol{U}^s\cdot i\boldsymbol{k}c'+\nabla_p(\dot{\boldsymbol{p}}'n\Psi)]=-\epsilon^2n^2[\nabla\cdot(e^{2i\omega t}e^{2i\boldsymbol{k}\cdot\boldsymbol{x}}\boldsymbol{u}'c')+\nabla_p\cdot(e^{2i\omega t}e^{2i\boldsymbol{k}\cdot\boldsymbol{x}}\dot{\boldsymbol{p}}'c')]. \tag{3.8}$$

In writing (3.8) we have used the continuity equation (3.4*b*). The linear stability problem is obtained by neglecting the terms of order ϵ^2 that appear on the right-hand side of (3.8). Thus, the stability problems involves a coupling between the bulk

particle density and fluid velocity fluctuations. The particle density fluctuations drive a bulk fluid motion, which in turn causes the particles to rotate affecting their sedimentation velocity and number density. This coupling is similar, but not identical, to the coupling investigated in §2 between the velocity disturbance caused by a single sedimenting particle and the pair probability.

We shall consider the base state in which the suspension is well mixed, i.e. the particle orientation distribution is isotropic, $\Psi = (4\pi)^{-1}$. Substituting (3.6*b*) and (3.7*b*) into (3.8) and neglecting terms of $O(\epsilon^2)$, we obtain the following integral equation for the particle density perturbation:

$$(\mathrm{i}\omega + \mathrm{i}\boldsymbol{k}\cdot\boldsymbol{U}^{\mathrm{s}})\,c' - \frac{3n\mathrm{i}}{4\pi\mu k^2}\left(\frac{\gamma^2-1}{\gamma^2+1}\right)p_i p_j k_i\left(\delta_{jk}-\frac{k_j k_k}{k^2}\right)f_k\int \mathrm{d}\boldsymbol{p}\,c' = 0. \tag{3.9}$$

In deriving (3.8) and (3.9) we have neglected any Brownian motion of the particles. Thus, there is no mechanism tending to dissipate particle density fluctuations, and we can only expect to obtain predictions of instability ($\omega_{\mathrm{I}} < 0$) or neutral stability ($\omega_{\mathrm{I}} = 0$) of the system considered. In this way the present analysis is similar to the inviscid stability analysis of plane shear waves (Drazin & Reed 1981), and as in that case we shall obtain a finite number (two) of discrete eigenvalues plus a continuous spectrum. If ω has a non-zero imaginary part or if ω is real and ω does not equal $-\boldsymbol{k}\cdot\boldsymbol{U}^{\mathrm{s}}(p)$ for any orientation $\boldsymbol{p}$, then we can divide (3.9) by $(\mathrm{i}\omega+\mathrm{i}\boldsymbol{k}\cdot\boldsymbol{U}^{\mathrm{s}})$ to obtain

$$c' = \frac{3n}{4\pi\mu k^2(\omega+\boldsymbol{k}\cdot\boldsymbol{U}^{\mathrm{s}})}\left(\frac{\gamma^2-1}{\gamma^2+1}\right)p_i p_j k_i\left(\delta_{jk}-\frac{k_j k_k}{k^2}\right)f_k\int \mathrm{d}\boldsymbol{p}\,c'. \tag{3.10}$$

Using a normalization condition, $\int \mathrm{d}\boldsymbol{p}\,c' = B(\boldsymbol{k})$, for the particle concentration perturbation (3.10) reduces to

$$c' = \frac{3nB}{4\pi\mu k^2(\omega+\boldsymbol{k}\cdot\boldsymbol{U}^{\mathrm{s}})}\left(\frac{\gamma^2-1}{\gamma^2+1}\right)p_i p_j k_i\left(\delta_{jk}-\frac{k_j k_k}{k^2}\right)f_k. \tag{3.11}$$

Here $B(\boldsymbol{k})$ is an arbitrary function of $\boldsymbol{k}$. The dispersion relation determining the discrete eigenvalues ω is obtained by substituting (3.11) into (3.9) to give

$$1 - \int \mathrm{d}\boldsymbol{p}\,\frac{3n}{4\pi\mu k^2(\omega+\boldsymbol{k}\cdot\boldsymbol{U}^{\mathrm{s}})}\left(\frac{\gamma^2-1}{\gamma^2+1}\right)p_i p_j k_i\left(\delta_{jk}-\frac{k_j k_k}{k^2}\right)f_k = 0. \tag{3.12}$$

When ω is real and $\omega = -\boldsymbol{k}\cdot\boldsymbol{U}^{\mathrm{s}}(\boldsymbol{p}_0)$ for some orientation $\boldsymbol{p}_0$, we cannot divide (3.9) by $(\mathrm{i}\omega+\mathrm{i}\boldsymbol{k}\cdot\boldsymbol{U}^{\mathrm{s}})$ as this would mean dividing by zero for $\boldsymbol{p} = \boldsymbol{p}_0$. However, in this case (3.9) has a solution in terms of generalized functions (Lighthill 1980):

$$c' = A\delta(\boldsymbol{p}-\boldsymbol{p}_0) + \frac{3nB}{4\pi\mu k^2(\omega+\boldsymbol{k}\cdot\boldsymbol{U}^{\mathrm{s}})}\left(\frac{\gamma^2-1}{\gamma^2+1}\right)p_i p_j k_i\left(\delta_{jk}-\frac{k_j k_k}{k^2}\right)f_k, \tag{3.13a}$$

for

$$\omega = -\boldsymbol{k}\cdot\boldsymbol{U}^{\mathrm{s}}(\boldsymbol{p}_0), \tag{3.13b}$$

where $A(\boldsymbol{k})$ is to be determined by the normalization condition $\int \mathrm{d}\boldsymbol{p}\,c' = B$. Note that the second term on the right-hand side of (3.13*a*) is a generalized function and its integral with respect to $\boldsymbol{p}$ is the same as the Cauchy principal value. The continuous spectrum of eigenvalues (3.13*b*) are all real. Thus, the solutions (3.13) are travelling waves with wave speeds equal to the sedimentation velocity $\boldsymbol{U}^{\mathrm{s}}(\boldsymbol{p}_0)$ for a particle of orientation $\boldsymbol{p}_0$. These travelling waves do not grow or decay with time, so the stability of the suspension is controlled by the discrete eigenvalues.

Returning our attention to the discrete eigenvalues, we define

$$k_3/k \equiv \cos\Theta,\ p_i k_i/k \equiv \cos\Theta',$$

and

$$p_3 \equiv \cos\Theta\cos\Theta' + \sin\Theta\sin\Theta'\cos\Phi.$$

For the present case, in which $\omega \neq -\boldsymbol{k}\cdot\boldsymbol{U}(\boldsymbol{p})$ for all $\boldsymbol{p}$, the integral with respect to Φ in (3.12) may be evaluated by contour integration over the unit circle in the complex plane to obtain

$$1-\frac{3nf}{2\mu k^2\beta_1}\left(\frac{\gamma^2-1}{\gamma^2+1}\right)\int \sin\Theta'\,\mathrm{d}\Theta' \times\left[1-\frac{1}{\left[1-\left(\frac{\beta_1 k\sin\Theta\sin\Theta'\cos\Theta'}{\omega+\beta_0 k\cos\Theta+\beta_1 k\cos\Theta\cos^2\Theta'}\right)^2\right]^{\frac{1}{2}}}\right]=0. \quad (3.14)$$

Although γ^2-1 and β_1 are both negative for oblate spheroids, the factor multiplying the integral in (3.14) is always positive. Thus, (3.14) can be written in terms of dimensionless variables as

$$1-\frac{1}{2k^{*2}}\int_{-1}^{1}\mathrm{d}\xi\left[1-\frac{1}{\left[1-\left(\frac{k^*\sin\Theta\xi[1-\xi^2]^{\frac{1}{2}}}{\omega^*+\beta_0^* k^*\cos\Theta+k^*\xi^2\cos\Theta}\right)^2\right]^{\frac{1}{2}}}\right]=0. \quad (3.15)$$

where

$$k^* = k\left[\frac{\mu\beta_1}{3nf}\left(\frac{\gamma^2-1}{\gamma^2+1}\right)\right]^{\frac{1}{2}}, \quad (3.16a)$$

$$\omega^* = \omega\left[\frac{\mu}{3nf\beta_1}\left(\frac{\gamma^2-1}{\gamma^2+1}\right)\right]^{\frac{1}{2}}, \quad (3.16b)$$

$$\beta_0^* = \frac{\beta_0}{\beta_1}, \quad (3.16c)$$

and

$$\xi = \cos\Theta'. \quad (3.16d)$$

Note that there is only one lengthscale and one timescale in this problem. The lengthscale is $(nl)^{-\frac{1}{2}}$ – the length at which buoyancy forces balance viscous forces. The timescale is the time $(nl)^{-\frac{1}{2}}\beta_1^{-1}$ required for a particle to sediment a distance comparable with the characteristic lengthscale $(nl)^{-\frac{1}{2}}$. For slender bodies, $\gamma \gg 1$, the characteristic lengthscale is $(nl)^{-\frac{1}{2}}[ln\,\gamma]^{\frac{1}{2}}$, however, it should be noted in this case that the diluteness approximations used in the preceding analysis are valid only if $nl^3 \ll 1$. The observation that the lengthscale of interest $(nl)^{-\frac{1}{2}}$ is much greater than the particle length l provides an *a posterior* justification of the use of (3.7*b*) to obtain the rotation rate $\dot{\boldsymbol{p}}$.

The maximum value that the integral in (3.14) can attain is 2. This sets an upper limit, $k^* = 1$, on the wavenumber for which discrete eigenfunctions may exist. This maximum wavenumber (minimum wavelength) is achieved in the limit $\omega^* \to 0$, when the waves are horizontal, i.e. $\Theta = \frac{1}{2}\pi$.

The behaviour of the eigenvalue ω^* in the limit of small wavenumber (large wavelength) may be obtained by expanding (3.15) in small k^*/ω^* and solving to give

$$\omega^* \approx \pm\mathrm{i}\frac{|\sin\Theta|}{(15)^{\frac{1}{2}}} - (\beta_0^* + \tfrac{3}{7})k^*\cos\Theta + O(k^{*2}) \quad (k^* \ll 1). \quad (3.17)$$

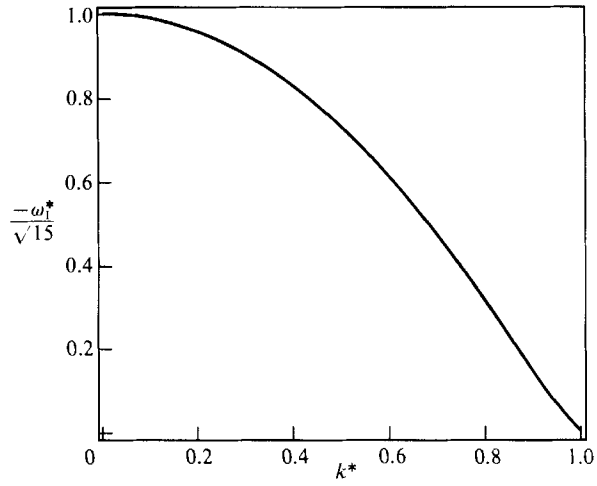

FIGURE 2. The imaginary part of the non-dimensional eigenvalue, ω_I^*, is plotted as a function of the non-dimensional wavenumber k^* for normal mode particle density perturbations with the wavenumber perpendicular to the direction of gravity i.e. $k_3^* = 0$.

From (3.17) it can be seen that there are growing solutions in the long wavelength limit, $k^* \to 0$. The fastest growing waves are those with horizontal wavenumbers, i.e. $\Theta = \frac{1}{2}\pi$, while the growth rate for waves with vertical wavenumbers, $\Theta = 0$, is zero. The latter result is not surprising, because purely vertical stratification does not drive any bulk fluid motion. The $O(k^*)$ term in (3.17) indicates that the waves travel in the direction of gravity with a non-dimensional velocity $(\beta_0^* + \frac{3}{7})\,\delta_{i3}$. In dimensional variables the wave speed is $(\beta_0 + \frac{3}{7}\beta_1)\,\delta_{i3}$. The waves travel because of the settling of the particles.

The discrete eigenvalues for waves with horizontal wavenumbers are purely imaginary, $\omega^* = i\omega_I^*$ for all wavenumbers k^*, where ω_I^* is given by

$$1 - \frac{1}{2k^{*2}} \int_{-1}^{1} dx \left[1 - \frac{1}{\left[1 + \dfrac{k^{*2}x^2(1-x^2)}{\omega_I^{*2}} \right]^{\frac{1}{2}}} \right] = 0. \tag{3.18}$$

Equation (3.18) was solved using Romberg integration with relative errors of $O(10^{-5})$ and secant iteration on ω_I^* again with $O(10^{-5})$ errors. In figure 2 we have plotted the growth rate ω_I^* of the disturbances versus the wavenumber. The growth rate increases monotonically with decreasing wavenumber from zero growth rate at the maximum wavenumber $k^* = 1$ to a growth rate of $(15)^{-\frac{1}{2}}$ at $k^* = 0$.

The result that the growth rate reaches a finite constant value as the wavenumber goes to zero may be rationalized in the following manner. The amplitude of the velocity field driven by a spatial particle density perturbation of fixed amplitude ϵB and wavenumber k^* increases like Bk^{*-2} as $k^* \to 0$ (cf. (3.6)). The shear rate and particle rotation rate grow like Bk^{*-1} (cf. (3.7)). This drives a particle density disturbance $c'(\boldsymbol{x}, \boldsymbol{p})$ (see (3.11)) in real and orientation space which is $O(Bk^{*-1})$, despite the fact that the purely spatial particle density fluctuation $\int d\boldsymbol{p}\, c'$ is normalized to B. In order that the orientation space particle density disturbance contributes to a growth in the spatial particle density disturbance the particles must translate half a wavelength (an $O(k^{*-1})$ distance) from a region of low to a region of

high particle density. Thus, the growth rate in the spatial particle density disturbance is $O(1)$ as $k^* \to 0$.

In the preceding linear stability analysis we found that the normal mode density perturbations with the maximum growth rate are those of arbitrarily large wavelength. This might be taken as an indication that particle density disturbances and velocity fluctuations which are the size of the settling vessel may be expected to arise in suspensions of non-spherical sedimenting particles. However, we do not believe that such long wavelength fluctuations will in fact develop.

The linear stability analysis applies only to perturbations of sufficiently small amplitude such that the particle orientation distribution is not greatly affected by the velocity disturbance. Thus, we require that the magnitude of $\epsilon n c'(\boldsymbol{x}, \boldsymbol{p})$ must be much smaller than the base state particle density $n\Psi(\boldsymbol{p})$. From (3.11) it can be seen that the magnitude of c' behaves like Bk^{*-1} as $k^* \to 0$. As a result, the small-amplitude restriction for the validity of the linear stability analysis is $\epsilon B \ll k^*$, where B is the amplitude of the disturbance. If this restriction is not satisfied then the nonlinear terms on the right-hand side of (3.8) cannot be neglected. The small-amplitude restriction is more stringent for perturbations of longer wavelengths, because as discussed previously longer wavelength spatial particle density fluctuations are more effective in driving a shear flow. Specifically, an $O(\epsilon B)$ real-space particle density disturbance of wavenumber k^* drives a shear rate, particle rotation rate, and orientation-space particle density disturbance which are each $O(\epsilon B k^{*-1})$.

The mechanism of the instability predicted here is illustrated in figure 3. A horizontal particle density wave induces a shear wave in which fluid is moving downward (upward) in regions of high (low) particle density. Each particle rotates in the local shear field surrounding it. However, the particle rotation rate is dilatational in particle orientation space, this dilatation resulting from the extensional component of the shear field. As a result, there is a net tendency for the particle density $c(\boldsymbol{x}, \boldsymbol{p})$ to increase at particle orientations which are within the 'extensional' quadrant – the quadrant in which the projection of the particle orientation into the plane of shear is within an angle $\frac{1}{4}\pi$ of the axis of extension for the extensional component of the shear field (see figure 3). The horizontal component of the settling velocity $\boldsymbol{U}^s(\boldsymbol{p})$ of particles with orientations in the 'extensional' quadrant is in the direction of increased particle density. Thus, the net effect of the shear wave is to increase the proportion of the particles that are oriented in such a way as to cause them to translate toward the regions of increased particle density; this clearly leads to growth of the particle density perturbation.

A different way of stating the small-amplitude restriction discussed above is that the change in orientation experienced by a particle as it translates through a wavelength of the disturbance must be small. If this condition is not satisfied, the particles will rotate in periodic orbits (Jeffery 1923) in the local shear flow. A particle undergoing steady rotation in a Jeffery orbit spends equal portions of its period in the 'extensional' and 'compressional' quadrants. Thus, the horizontal component of the time-averaged particle velocity will go to zero as $\epsilon B k^{*-1} \to \infty$ so that the particle experiences many periods of the Jeffery orbit in the time it takes to transverse half a wavelength from a region of low density to one of high density. Thus, we conclude that the growth rates of perturbations whose amplitudes are large compared with their wavenumber, $1 \gg \epsilon B > k^*$, decrease with decreasing wavenumber (increasing wavelength). However, our linear stability analysis indicates that the suspension is stable to wavenumbers $k^* \geqslant 1$. Therefore, we expect that ultimately finite-amplitude

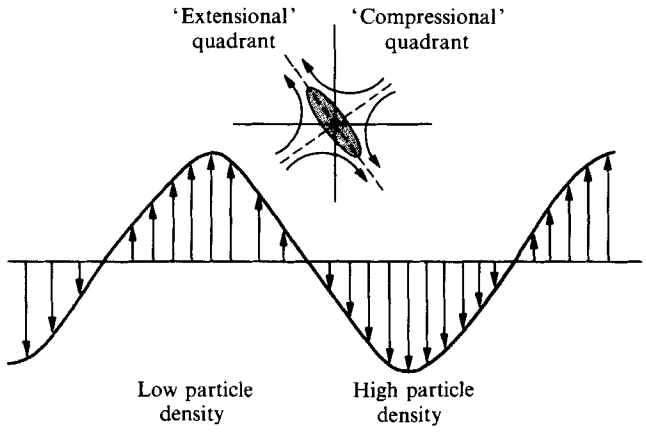

FIGURE 3. Schematic illustration of the instability mechanism. A horizontal normal mode particle density perturbation drives a vertical shear flow. The streamlines of the extensional component of the local, linear shear field are illustrated. The flow field tends to increase the particle density of orientations within the 'extensional quadrant' – the quadrant consisting of orientations whose projection into the plane of shear is within an angle of $\frac{1}{4}\pi$ of the extensional axis. A particle is drawn in the most favoured orientation. Particles with orientations in the extensional quadrant sediment with a horizontal component in the direction of increasing particle density, thus causing a growth of the particle density perturbation.

density fluctuations with dimensionless wavenumber $k^* \approx O(1)$ or, equivalently, dimensional wavelengths of order $(nl)^{-\frac{1}{2}}$ will predominate.

We have seen that suspensions of spheroidal particles are unstable to particle density perturbations with wavenumbers in the range $0 \leqslant k^* < 1$. The type of normal-mode perturbation with the maximum growth rate is apparently a wave of horizontal wavenumber and $k^* \to 0$. The growth rate of the instability decreases as $\gamma \to 1$, i.e. as the particles become spherical. Note that when $|\gamma - 1| < \phi$ two particle interactions will have a larger effect on the sedimentation of velocity than does the particle orientation. Here, ϕ is the particle volume fraction. The stability of suspensions of spherical particles is examined in §4.

4. Stability analysis for suspensions of spheres

In this section we consider the stability of a dilute, homogeneous, monidisperse suspension of spheres in the absence of inertial effects to small particle number density perturbations. In §3, a sedimenting suspension of non-spherical axisymmetric particles with fore–aft symmetry was shown to be unstable to such perturbations. The mechanism that led to that instability involved a coupling between the particles' setttling velocities, their orientations, and the fluid motion induced by the particle density perturbations. The fluid motion induced by a particle density perturbation caused the particles to rotate such that more particles were aligned with the extensional than the compressional axis of the local shear field. Because the velocity of the particles depends on their orientation, this change in particle orientation induced a net particle flux toward regions of high particle density, thus, leading to the instability.

If one neglected particle interactions entirely in a suspension of spheres (as was done in the stability analysis for spheroids), there would be no coupling between the particles' velocities and their orientation, and thus no comparable mechanism of

instability. However, if we consider interactions between pairs of particles, a coupling similar to that treated in §3 for spheroids exists. A pair of particles settles relative to the surrounding fluid with a velocity which depends on the relative position of the particles. This relative position is, in turn, influenced by the velocity field created by the particle density perturbations.

In many ways the stability analysis here will be similar to that in §3, however an important distinction between the orienting behaviours of a pair of spheres and a spheroid will lead to stability in the present study of suspensions of spheres, where we found a suspension of spheroids to be unstable in §3. The essential difference in the physics of the two cases is discussed in detail at the conclusion of this section. A dilute suspension of slightly non-spherical particles may be stable like the suspensions of spheres treated here, or unstable like the suspension spheroid in §3, depending on the relative magnitude of $|\gamma^2-1|$ and the volume fraction ϕ. If $|\gamma^2-1| \ll \phi$, then the present analysis applies, whereas the analysis in §3 applies, when $\phi \ll |\gamma^2-1|$.

In the present instance, we are interested in the concentration or number density $c_2(\boldsymbol{x}, \boldsymbol{r})$ of pairs of particles located at positions $\boldsymbol{x}-\frac{1}{2}\boldsymbol{r}$ and $\boldsymbol{x}+\frac{1}{2}\boldsymbol{r}$. The pair concentration satisfies the conservation equation:

$$\frac{\partial c_2}{\partial t}+\boldsymbol{\nabla}\cdot(\boldsymbol{U}c_2)+\boldsymbol{\nabla}_r\cdot(\dot{\boldsymbol{r}}c_2)=0, \tag{4.1}$$

where $\boldsymbol{\nabla}$ and $\boldsymbol{\nabla}_r$ are the Nablé operators with derivatives taken with respect to $\boldsymbol{x}$ and $\boldsymbol{r}$, respectively, $\boldsymbol{U}$ is the velocity of the pair's centre of mass, and $\dot{\boldsymbol{r}}$ is the velocity of the particle at $\boldsymbol{x}+\frac{1}{2}\boldsymbol{r}$ relative to the one at $\boldsymbol{x}-\frac{1}{2}\boldsymbol{r}$.

Note that in writing (4.1) we have neglected any possible Brownian or hydrodynamic diffusion of the particles. As a result, there is no dissipative mechanism, (4.1) will always have travelling wave solutions, and one can only expect to obtain neutral stability or instability from the present analysis.

We shall consider pairs of particles that are sufficiently close together that the fluid velocity may be approximated by a linear shear flow on lengths of order r. It will be seen that the suspensions's stability is controlled by pairs whose separation $r \approx O(a)$, so that the aforementioned approximation is valid for particle density perturbations whose wavenumbers satisfy $k^{-1} \gg a$. The criterion $k^{-1} \gg a$ is also necessary for the validity of our treatment of the pair concentration c_2 as a continuum variable.

In the presence of such slowly varying fluid velocity disturbances, the velocity $\boldsymbol{U}$ of the pair's centre of mass is simply the sum of the average fluid velocity $\langle \boldsymbol{u} \rangle$ and the sedimentation velocity $\boldsymbol{U}^0$ of the pair in a quiescent fluid. This sedimentation velocity is given by:

$$\boldsymbol{U}^0 = F\boldsymbol{U}^s + G\boldsymbol{r}\frac{\boldsymbol{r}\cdot\boldsymbol{U}^s}{r^2}, \tag{4.2}$$

where $F+G$ and F are inverse resistance coefficients for the motion of two identical particles parallel and perpendicular to their line of centres, respectively (Batchelor 1972; Stimson & Jeffery 1926; Goldman, Cox & Brenner 1966). F and G are functions of r and are always positive.

The relative velocity of a pair in the presence of a velocity disturbance for which $k^{-1} \gg a$ is the same as that of a pair of neutrally buoyant spheres in a linear shear field. This relative velocity is (Batchelor & Green 1972):

$$\dot{r}_i = \frac{\partial \langle u_i \rangle}{\partial x_j} r_j - \left[A\frac{r_i r_j}{r^2} + B\left(\delta_{ij} - \frac{r_i r_j}{r^2}\right)\right] E_{jk} r_k, \tag{4.3a}$$

where

$$\boldsymbol{E} = \tfrac{1}{2}[\boldsymbol{\nabla}\langle \boldsymbol{u} \rangle + \boldsymbol{\nabla}\langle \boldsymbol{u} \rangle^{\dagger}], \tag{4.3b}$$

A and B are positive functions of r tabulated by Batchelor & Green (1972), and $A > B$ for all r. Another useful relation is

$$\nabla_r \cdot \dot{\boldsymbol{r}} = W\frac{\boldsymbol{r}\cdot\boldsymbol{E}\cdot\boldsymbol{r}}{r^2} = W\frac{\boldsymbol{r}\cdot\nabla\langle\boldsymbol{u}\rangle\cdot\boldsymbol{r}}{r^2}, \tag{4.4}$$

where $W = r(\mathrm{d}A/\mathrm{d}r) + 2(A-B)$ is tabulated by Batchelor (1977) and is always positive.

To calculate the average fluid velocity field used in (4.3) and (4.4), we shall use a point-particle approximation, which is valid when $k^{-1} \gg a$ so that most of the particles causing the fluid velocity disturbance at $\boldsymbol{x}$ are a large distance away from the pair. Taking the unconditional ensemble average of (3.3) and (3.2b) gives:

$$-\mu\nabla^2\langle\boldsymbol{u}\rangle + \nabla\langle p\rangle = \frac{\boldsymbol{f}}{n}\int \mathrm{d}\boldsymbol{r}[c_2(\boldsymbol{x}+\tfrac{1}{2}\boldsymbol{r},\boldsymbol{r}) + c_2(\boldsymbol{x}-\tfrac{1}{2}\boldsymbol{r},\boldsymbol{r}) - 2n^2\Omega(\boldsymbol{r})], \tag{4.5a}$$

$$\nabla\cdot\langle\boldsymbol{u}\rangle = 0. \tag{4.5b}$$

Provided that the wavelength of the instability is sufficiently long, i.e. $k^{-1} \gg r$, (4.5a) reduces to

$$-\mu\nabla^2\langle\boldsymbol{u}\rangle + \nabla\langle p\rangle \approx \frac{2\boldsymbol{f}}{n}\int \mathrm{d}\boldsymbol{r}[c_2(\boldsymbol{x},\boldsymbol{r}) - n^2\Omega(\boldsymbol{r})]. \tag{4.6}$$

In (4.5a) and (4.6), $\Omega(\boldsymbol{r})$ is the pair distribution function averaged over the volume of the system, and $\Omega(\boldsymbol{r})$ has been normalized such that $\Omega \to 1$ as $r \to \infty$.

The base state for our stability analysis is a homogeneous suspension, for which the pair concentration is $c_2(\boldsymbol{x},\boldsymbol{r}) = n^2\Omega(\boldsymbol{r})$. This spatially homogeneous particle density drives no average velocity in (4.6), so that $\langle\boldsymbol{u}\rangle = 0$. Because there is no average velocity, the relative velocity $\dot{\boldsymbol{r}}$ is zero, and the pair conservation equation (4.1) is satisfied by this base state.

We consider a normal-mode pair concentration perturbation of small amplitude ϵ, i.e.

$$c_2(\boldsymbol{x},\boldsymbol{r},t) = n^2[\Omega(\boldsymbol{r}) + \epsilon c_2'(\boldsymbol{k},\omega,\boldsymbol{r})\,\mathrm{e}^{\mathrm{i}\omega t}\,\mathrm{e}^{\mathrm{i}\boldsymbol{k}\cdot\boldsymbol{x}}]. \tag{4.7}$$

The suspension will be unstable if there are perturbations for which the frequency ω has a negative imaginary part.

The pair density perturbation drives a small fluid velocity:

$$\langle\boldsymbol{u}\rangle = \epsilon n^2\boldsymbol{u}'\,\mathrm{e}^{\mathrm{i}\omega t}\,\mathrm{e}^{\mathrm{i}\boldsymbol{k}\cdot\boldsymbol{x}}. \tag{4.8a}$$

Substituting (4.8a) and (4.7) into (4.6) gives:

$$\boldsymbol{u}'(\boldsymbol{k},\omega) = \frac{\boldsymbol{f}\cdot\left(\boldsymbol{I}-\dfrac{\boldsymbol{kk}}{k^2}\right)}{\mu k^2}\int \mathrm{d}\boldsymbol{r}\,c_2'(\boldsymbol{k},\omega,\boldsymbol{r}). \tag{4.8b}$$

This small fluid velocity in turn induces a small relative velocity between the pair of particles

$$\dot{\boldsymbol{r}} = \epsilon n^2\dot{\boldsymbol{r}}'\,\mathrm{e}^{\mathrm{i}\omega t}\,\mathrm{e}^{\mathrm{i}\boldsymbol{k}\cdot\boldsymbol{x}}, \tag{4.9}$$

where $\dot{\boldsymbol{r}}'$ is simply given by (4.3) with $\nabla\langle\boldsymbol{u}\rangle$ replaced by $\boldsymbol{ku}'$.

Substituting (4.7), (4.8) and (4.9) into the pair conservation equation (4.1) and using the continuity equation (4.5b), we obtain

$$\begin{aligned}\epsilon n^2\,\mathrm{e}^{\mathrm{i}\omega t}\,\mathrm{e}^{\mathrm{i}\boldsymbol{k}\cdot\boldsymbol{x}}[\mathrm{i}\omega c_2' + \mathrm{i}\boldsymbol{U}^0\cdot\boldsymbol{k}c_2' + \nabla_r\cdot(\dot{\boldsymbol{r}}'n^2\Omega)] \\ = -\epsilon^2 n^4[\nabla\cdot(\mathrm{e}^{2\mathrm{i}\omega t}\,\mathrm{e}^{2\mathrm{i}\boldsymbol{k}\cdot\boldsymbol{x}}\boldsymbol{u}'c_2') + \nabla_r\cdot(\mathrm{e}^{2\mathrm{i}\omega t}\,\mathrm{e}^{2\mathrm{i}\boldsymbol{k}\cdot\boldsymbol{x}}\dot{\boldsymbol{r}}'c_2')].\end{aligned} \tag{4.10}$$

The linear stability problem is obtained by neglecting the terms of order ϵ^2, which appear on the right-hand side of (4.10). This stability problem is similar to that for a sedimenting suspension of spheroids treated in §3, the distinction being that here the pair concentration, relative velocity, etc. replaces the spheroid concentration, rotational velocity, etc. Here, the stability problem involves a coupling between the pair concentration and fluid velocity fluctuations.

We shall consider the base state in which the suspension is random, i.e. the pair distribution function $\Omega(\boldsymbol{r}) = 1$ for all $r \geqslant 2a$ independent of relative position. Substituting (4.2), (4.4) and (4.8) into (4.10), and neglecting the terms of $O(\epsilon^2)$, we obtain the following integral equation for the pair concentration perturbation:

$$(\mathrm{i}\omega + \mathrm{i}\boldsymbol{k}\cdot\boldsymbol{U}^0)\, c_2' + \frac{\mathrm{i}n^2 W}{2\mu k^2}\frac{r_i r_j}{r^2} k_i \left(\delta_{jk} - \frac{k_j k_k}{k^2}\right) f_k \int \mathrm{d}\boldsymbol{r}\, c_2' = 0. \tag{4.11}$$

This stability analysis like the similar analysis in §3 involves no dissipative mechanism and again we obtain a finite number (two) of discrete eigenvalues plus a continuous spectrum. By a procedure analogous to that described in §3, we find the continuous spectrum of eigenfunctions and eigenvalues to be:

$$c_2' = A\delta(\boldsymbol{r} - \boldsymbol{r}_0) + \frac{n^2 BW}{2\mu k^2(\omega + \boldsymbol{U}^0\cdot\boldsymbol{k})}\frac{r_i r_j}{r^2} k_i \left(\delta_{jk} - \frac{k_j k_k}{k^2}\right) f_k,$$

for all

$$\omega = -\boldsymbol{k}\cdot\boldsymbol{U}^0(\boldsymbol{r}_0), \tag{4.12a, b}$$

where the constant A is determined from the normalization condition $\int \mathrm{d}\boldsymbol{r}\, c_2' = B(\boldsymbol{k})$. The second term on the right-hand side of (4.12a) is a generalized function and its integral with respect to $\boldsymbol{r}$ is defined to be the Cauchy principal value (Lighthill 1980). The continuous spectrum of eigenvalues are real, corresponding to travelling waves of constant amplitude with wave speeds equal to the sedimentation velocity $\boldsymbol{U}^0(\boldsymbol{r}_0)$ of a pair of spheres with relative position $\boldsymbol{r}_0$.

The discrete eigenfunctions are of the form (cf. §3):

$$c_2' = \frac{n^2 WB}{2\mu k^2(\omega + \boldsymbol{U}^0\cdot\boldsymbol{k})}\frac{r_i r_j}{r^2} k_i \left(\delta_{jk} - \frac{k_j k_k}{k^2}\right) f_k, \tag{4.13}$$

and the dispersion relation for ω obtained by substituting (4.13) into (4.11) is:

$$1 + \int \mathrm{d}\boldsymbol{r}\, \frac{n^2 W}{2\mu k^2(\omega + \boldsymbol{U}^0\cdot\boldsymbol{k})}\frac{r_i r_j}{r^2} k_i \left(\delta_{jk} - \frac{k_j k_k}{k^2}\right) f_k = 0. \tag{4.14}$$

We now define $k_3/k \equiv \cos\Theta$, $r_i k_i/rk \equiv \cos\Theta'$, and

$$r_3/r \equiv \cos\Theta\cos\Theta' + \sin\Theta\sin\Theta'\cos\phi,$$

where r_3 and k_3 are the components of $\boldsymbol{r}$ and $\boldsymbol{k}$ in the direction of the gravitational acceleration. When ω is not part of the continuous spectrum of eigenvalues, i.e. $\omega \neq -\boldsymbol{k}\cdot\boldsymbol{U}^0(\boldsymbol{r})$ for all $\boldsymbol{r}$, the integral with respect to ϕ in (4.14) may be evaluated by contour integration over the unit circle in the complex plane to obtain

$$1 + \frac{\pi n^2 f}{\mu k^2 U^s}\int_2^\infty r^2\,\mathrm{d}r\,\frac{W}{G}\int_0^\pi \sin\Theta'\,\mathrm{d}\Theta' \times\left[1 - \frac{1}{\left[1 - \left(\dfrac{U^s Gk\sin\Theta\sin\Theta'\cos\Theta'}{\omega + U^s Fk\cos\Theta + U^s Gk\cos\Theta\cos^2\Theta'}\right)^2\right]^{\frac{1}{2}}}\right] = 0. \tag{4.15}$$

Equation (4.15) can be written in terms of dimensionless variables as

$$1+\frac{1}{2k^{*2}}\int_2^\infty r^{*2}\,\mathrm{d}r^*\frac{W}{G}\int_{-1}^{1}\mathrm{d}\xi\left[1-\frac{1}{\left[1-\left(\frac{k^*G\sin\Theta\xi[1-\xi^2]^{\frac{1}{2}}}{\omega^*+k^*\cos\Theta[F+G\xi^2]}\right)^2\right]^{\frac{1}{2}}}\right]=0, \quad (4.16)$$

where

$$k^*\equiv k\left[\frac{\mu U^s}{2\pi n^2 f a^3}\right]^{\frac{1}{2}}, \quad (4.17a)$$

$$\omega^*\equiv \omega\left[\frac{\mu}{2\pi n^2 f a^3 U^s}\right]^{\frac{1}{2}}, \quad (4.17b)$$

$$r^*\equiv r/a, \quad (4.17c)$$

and

$$\xi\equiv\cos\Theta'. \quad (4.17d)$$

Note that the wavenumber k^* is non-dimensionalized with the reciprocal of the $O(a\phi^{-1})$ wavelength at which buoyancy forces associated with changes in the pair concentration balance viscous forces, and the frequency ω^* is non-dimensionalized with the reciprocal of the $O(a\phi^{-1}(U^s)^{-1})$ time required for a pair of particles to fall through this length.

The crucial difference between the expression (4.16) for the eigenvalues in the stability analysis for a suspension of spheres and the analogous expression (3.15) in the spheroids stability analysis is the difference in sign of the second terms on the right-hand sides of these two expressions. This distinction has the consequence that, while the eigenvalues are complex and the suspension unstable in the spheroids case, the eigenvalues are real and the suspension stable in the present case of spherical particles. The aforementioned sign difference results from the fact that the orientation space dilatation of the spheroid's rotation rate is negative in the extensional quadrant and positive in the compressional quadrant (cf. (2.4)), while the dilatation of the relative velocity of the pair of spheres is positive in the extensional quadrant and negative in the compressional quadrant (cf. (4.4)).

A physical understanding of the difference in the stability of the two types of suspension may be gained by comparing figures 3 and 4. In both cases the density differences resulting from a normal-mode perturbation in the number density of particles drives a spatially oscillating shear flow. The spheroidal particles in figure 3 tend to align in the extensional quadrant of the shear field with the consequence that they translate in the direction of increasing number density, making the suspension unstable. However, the preferred orientation for pairs of spheres is in the compressional quadrant, so they tend to migrate towards regions of low particle density, making the suspension stable, cf. figure 4. As noted above there is no dissipative mechanism, so the suspension is only neutrally stable.

The simplest case is that of 'horizontal' waves, i.e. perturbations whose wavenumber is perpendicular to gravity. In this case, $\Theta=\frac{1}{2}\pi$ and (4.16) reduces to

$$1+\frac{1}{2k^{*2}}\int_2^\infty r^{*2}\,\mathrm{d}r^*\frac{W}{G}\int_{-1}^{1}\mathrm{d}\xi\left[1-\frac{1}{\left[1-\left(\frac{k^{*2}G^2\xi^2[1-\xi^2]}{\omega^{*2}}\right)\right]^{\frac{1}{2}}}\right]=0. \quad (4.18)$$

There are two solutions ω^* of (4.18) for each value of k^* and both solutions are real. If ω^* is a solution of (4.18) so is its negative, $-\omega^*$. The positive eigenvalue is plotted as a function of k^* in figure 5.

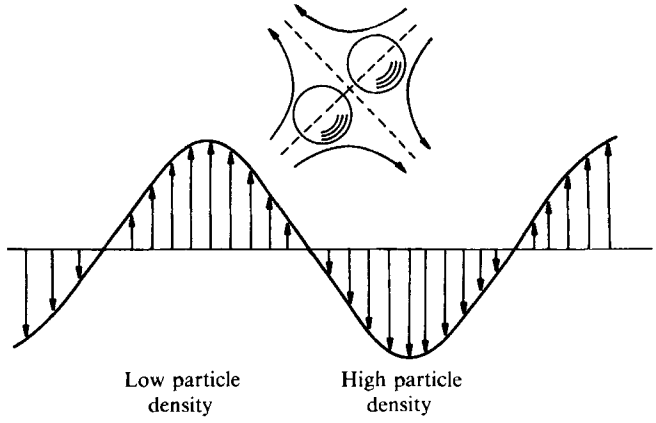

FIGURE 4. Schematic illustration of the mechanism leading to stability in a suspension of spheres. A normal mode perturbation with horizontal wavenumber drives a vertical shear flow. The streamlines of the extensional component of the local, linear shear field are illustrated. The flow field tends to increase the pair density for relative positions in the 'compressional' quadrant – the quadrant consisting of relative positions whose projection into the plane of shear are within an angle $\frac{1}{4}\pi$ of the compressional axis. Pairs with such relative positions sediment with a horizontal component in the direction of decreasing particle density, leading to stability of the homogeneous suspension.

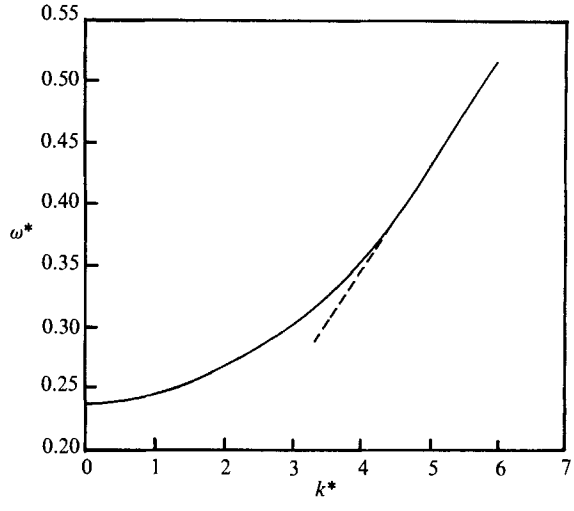

FIGURE 5. The positive, non-dimensional eigenvalue ω^* is plotted as a function of the non-dimensional wavenumber k^* for horizontal waves, i.e. $\Theta = \frac{1}{2}\pi$. The negative eigenvalue is simply the negative of the eigenvalue plotted. The eigenvalues for negative k^* are given by $\omega^*(-k^*) = -\omega^*(k^*)$. The asymptotes are $\omega^* \to 0.2312$ as $k^* \to 0$ and $\omega^*/k^* \to 0.08507$ as $k^* \to \infty$, cf. (4.19) and (4.20).

The possibility of complex eigenvalues for horizontal waves, $\Theta = \frac{1}{2}\pi$, can be excluded by the following argument. If ω^* is purely imaginary, then the second term in the integrand in (4.18) is always real and greater than -1. As a result the integrand and the integral are positive and no equality is possible. Thus, there are no purely imaginary eigenvalues. The only other alternative is that ω^* has non-zero real and imaginary parts. In this case, $(k^*/\omega^*)^2$ is complex and the integrand is complex. Thus, the equality in (4.18) can only be satisfied if the imaginary contributions to the

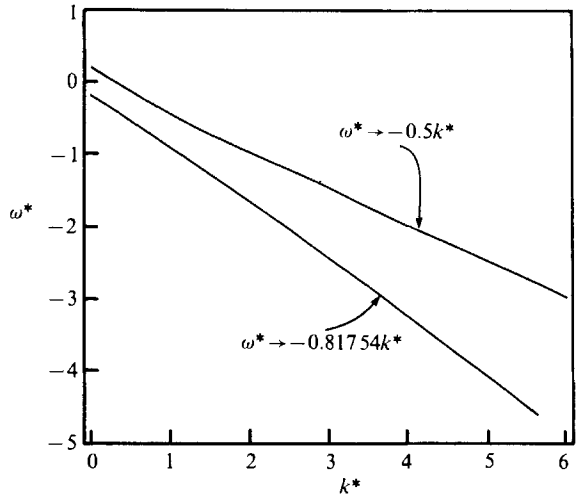

FIGURE 6. The non-dimensional eigenvalues ω^* are plotted as a function of non-dimensional wavenumber k^* for the case where the angle between the wavenumber vector and the direction of gravity is $\Theta = \frac{1}{3}\pi$. The eigenvalues for negative values of k^* are given by $\omega^*(-k^*) = -\omega^*(k^*)$. The asymptotes for the eigenvalues are $\omega^* \to \pm 0.2005$ as $k^* \to 0$, and $\omega^*/k^* \to -0.5$ and $\omega^*/k^* \to -0.8175$ as $k^* \to \infty$, cf. (4.19) and (4.20).

integral corresponding to different points in the range of integration cancel. Consider, first, the case in which $(k^*/\omega^*)^2$ is the upper half plane. The quantity $1 - k^{*2}G^2\xi^2(1-\xi^2)/\omega^{*2}$ is then in the lower half plane for all r and ξ. The denominator of the second term is also always in the lower half plane since the branch cut for the square root is along the negative real axis. Thus, this second term is always in the upper plane and all the imaginary contributions to the integral are positive. Thus, the equality in (4.18) cannot hold for any value of $(k^*/\omega^*)^2$ with a positive real part. An analogous argument can be used to preclude the possibility of a solution for $(k^*/\omega^*)^2$ with a negative real part. This completes the proof that all the eigenvalues are real.

Although it is not straightforward to extend this simple argument to the case of non-horizontal waves, $\Theta \neq \frac{1}{2}\pi$, we believe that there are again only real solutions in the latter case. To test this supposition, we have computed the eigenvalues for the case $\Theta = \frac{1}{3}\pi$. The two eigenvalues, which are real but, unlike those for horizontal waves, are not negatives of one another, are plotted in figure 6.

The asymptotic behaviour of the eigenvalues in the limit of small wavenumber may be found by expanding the integrand in (4.16) to give

$$\omega^* \approx \pm \frac{1}{(15)^{\frac{1}{2}}} \left(\int_2^\infty r^2 WG \, \mathrm{d}r \right)^{\frac{1}{2}} \sin\Theta + O(k^*) \approx \pm 0.2312 \sin\Theta + O(k^*) \quad (k^* \ll 1). \tag{4.19}$$

For every value of Θ, there is a finite range of the real k^*/ω^* axis over which there are no eigensolutions, because in this range the integrand in (4.16) is singular for some r and ξ. The large k^* asymptotes of the eigenvalues correspond to the endpoints of this range. These asymptotes may be found after considerable algebra to be:

$$\frac{k^*}{\omega^*} \approx \frac{-(2F_\mathrm{m} + G_\mathrm{m})\cos\Theta - G_\mathrm{m}}{2F_\mathrm{m}(F_\mathrm{m} + G_\mathrm{m})\cos^2\Theta - \frac{1}{2}G_\mathrm{m}^2 \sin^2\Theta} \quad (\kappa^* \to \infty), \tag{4.20a}$$

$$\frac{k^*}{\omega^*} \approx \max\left[\frac{-(2F_m+G_m)\cos\Theta+G_m}{2F_m(F_m+G_m)\cos^2\Theta-\frac{1}{2}G_m^2\sin^2\Theta}, -\cos\Theta\right] \quad (k^*\to\infty), \quad (4.20b)$$

where $F_m \equiv F(2)$ and $G_m \equiv G(2)$ are the maximum values of the functions F and G.

Thus, we have found only real eigenvalues in the stability analysis for a suspension of spheres, indicating that such a suspension is neutrally stable to particle number density perturbations.

5. Conclusions

In this paper we have examined the effects of hydrodynamic interactions between non-spherical axisymmetric particles with fore–aft symmetry on the structure of a sedimenting suspension. As noted in §1, many system properties, such as the mean and variance of the particle velocity and the particle diffusivity depend on the size of the sedimenting system in a random suspension with uniform probability. Therefore, it of interest to examine the structure of an actual sedimenting suspension. In particular one would like to know whether structural effects allow one to determine the aforementioned system properties without reference to the macroscale dimension of the system.

In §2, we found that interactions between spheroidal particles in a homogeneous suspension lead to an increase in the number density of neighbouring particles over a large lengthscale. This tendency for particles to agglomerate suggests that a homogeneous suspension is unstable to particle density perturbations. In §3 we confirmed via a linear stability analysis that such a suspension is indeed unstable. Unfortunately, as a result, one cannot hope to calculate the properties of a sedimenting suspension of spheroids based on the assumption of statistical homogeneity. The possibility of a similar instability occurring in a suspension of spheres was precluded by the stability analysis in §4.

From the analysis presented in §3, we expect the convective motions associated with the instability to occur on lengthscales of order $(nl)^{-\frac{1}{2}}$. As the number density increases it follows that the expected wavelength of the instability will decrease so that in a non-dilute suspension this wavelength would be of the same order as the particle size and the convective motion associated with the instability would be difficult to distinguish from the random motion of the particles. Thus, in order to observe this instability most easily, one should examine dilute sedimenting suspensions.

There is currently some interest in numerical simulations of sedimenting suspensions (cf. Brady & Durlofsky 1988). Our prediction of convective motions on a lengthscale $(nl)^{-\frac{1}{2}}$ implies that in order to simulate accurately the dynamics of a three-dimensional, dilute sedimenting suspension of non-spherical particles one needs a 'box' whose linear dimension is much larger than $(nl)^{-\frac{1}{2}}$ or, alternatively, a number N of particles that is large compared to $(nl^3)^{-\frac{1}{2}}$. It follows that the number of particles required to accurately simulate the sedimentation process will increase with decreasing number density.

It should be noted that the fastest growing wavelength $(nl)^{-\frac{1}{2}}$ of the instability will be, in general, much smaller than the size of the sedimenting system. The primary difficulty in observing this instability lies in differentiating the random convective motion associated with the instability, which occurs on lengths of $O((nl)^{-\frac{1}{2}})$, from the random motion of individual particles. However, there are a number of observations, which may be made relatively easily and yet indicate the existence of the instability.

For instance, the convective motion may lead to an average sedimentation velocity which is larger than the maximum possible value for a particle in a quiescent fluid. Thus, accurate measurement of the sedimentation velocity may indicate the presence of this instability. The presence of the convective motion may also be confirmed by comparing measurements of the sedimenting particles' velocity variance in a dilute suspension with scalings based on the magnitude of the convective motion associated with particle density variations on the lengthscale $(nl)^{-\frac{1}{2}}$.

One of the authors (D.L.K.) gratefully acknowledges financial support from the donors of the Petroleum Research Fund administered by the American Chemical Society and from National Science Foundation Grant no. MSME-8857565.

REFERENCES

BATCHELOR, G. K. 1972 Sedimentation in a dilute dispersion of spheres. *J. Fluid Mech.* **52**, 245–268.

BATCHELOR, G. K. 1977 The effect of Brownian motion on the bulk stress in a suspension of spherical particles. *J. Fluid Mech.* **83**, 97–117.

BATCHELOR, G. K. & GREEN, J. T. 1972 The hydrodynamic interactions of two small freely-moving spheres in a linear flow field. *J. Fluid Mech.* **56**, 375–400.

BRACEWELL, R. N. 1978 *The Fourier Transform and its Applications*, 2nd edn, p. 253. McGraw-Hill.

BRADY, J. F. & DURLOFSKY, L. J. 1988 The sedimentation rate of disordered suspensions. *Phys. Fluids* **31**, 717–727.

BRETHERTON, F. P. 1962 The motion of rigid particles in a shear flow at low Reynolds number. *J. Fluid Mech.* **14**, 284–304.

CAFLISCH, R. E. & LUKE, H. C. 1985 Variance in the sedimentation speed of a suspension. *Phys. Fluids* **28**, 759–760.

DRAZIN, P. G. & REID, W. H. 1981 *Hydrodynamic Stability*, pp. 124–153. Cambridge University Press.

GOLDMAN, A. J., COX, R. G. & BRENNER, H. 1966 The slow motion of two identical arbitrarily oriented spheres through a viscous fluid. *Chem. Engng Sci.* **21**, 1151–1170.

HAPPEL, J. & BRENNER, H. 1965 *Low Reynolds Number Hydrodynamics*, pp. 220–232. Prentice Hall.

JEFFERY, G. B. 1923 The motion of ellipsoidal particles immersed in a viscous fluid. *Proc. R. Soc.* A **102**, 161–179.

KIM, S. 1985 Sedimentation of two arbitrarily oriented spheroids in a viscous fluid. *Intl J. Multiphase Flow* **11**, 699–712.

LIGHTHILL, M. J. 1980 *An Introduction to Fourier Analaysis and Generalized Functions*, pp. 35–40. Cambridge University Press.

OBERBECK, A. 1876 Ueber stationare Flüssigkeitsbewegungen mit Berücksichtigung der inneren Reibung. (On steady state fluid flow and the calculation of the drag.) *J. reine angew. Math.* **81**, 62–80.

SAFFMAN, P. G. 1973 On the settling speeds of free and fixed suspensions. *Stud. Appl. Maths* **52**, 115–127.

SHAQFEH, E. S. G. & KOCH, D. L. 1988 The effect of hydrodynamic interactions on the orientation of axisymmetric particles flowing through a fixed bed of spheres or fibers. *Phys. Fluids* **31**, 728–743.

STIMSON, M. & JEFFERY, G. B. 1926 The motion of two spheres in a viscous fluid. *Proc. R. Soc.* A **111**, 110.